# Magnetic properties and hyperfine interactions in amorphous Fe-Zr alloys

K. M. Unruh* and C. L. Chien
*Department of Physics, The Johns Hopkins University, Baltimore, Maryland 21218*
(Received 24 May 1984)

Amorphous $Fe_xZr_{100-x}$ ($20 \leq x \leq 93$) samples were prepared with a high-rate sputtering technique and systematically studied using $^{57}$Fe Mössbauer spectroscopy. Below a critical Fe concentration of $x_c \approx 45$, magnetic order does not occur due to the loss of the Fe moment. Instead, superconductivity with reasonably high transition temperatures appears. Above $x_c$, a maximum in the magnetic ordering temperature ($T_c$) was found at $x_p \simeq 85$. At higher Fe concentrations, $T_c$ decreased and an extrapolation to $x = 100$ yielded an estimate of $T_c$ in pure amorphous Fe of about 200 K. Measurements of the effective hyperfine field ($H_{\text{eff}}$) and the distribution of hyperfine fields [$P(H)$] were also carried out. The effective hyperfine field was found to increase monotonically with the Fe concentration, unlike the values of $T_c$, and therefore indicates a monotonically increasing value of the Fe moment. These characteristics are consistent with a localized-moment description of the magnetism in which an antiferromagnetic exchange component appears at high Fe concentrations. The concentration dependence of the electric quadrupole splitting and the isomer shift were also obtained. The former shows a large difference between Fe-rich and Zr-rich samples. In the latter case, the semiempirical model of Miedema and van der Woude was found to be in qualitative agreement with the data.

## I. INTRODUCTION

The liquid-quench and the vapor-deposition techniques are the two methods most generally used to produce amorphous alloys.[1,2] While the liquid-quench method can produce large amounts of material, it is in general only successful for compositions near where deep eutetics in the alloy phase diagram are found. The vapor-deposition method, achieving much higher quenching rates, suffers from no such restrictions and is capable of producing amorphous alloys over a much wider range of compositions. For studies in which the composition dependence of the various properties of an alloy system is desired, the vapor-deposition method is much to be preferred over the liquid-quench method as a technique for sample preparation.

In the case of the metal-metal system Fe-Zr, the existence of two eutectics in the binary phase diagram has made it possible to liquid-quench amorphous alloys near the compositions $Fe_{25}Zr_{75}$ and $Fe_{90}Zr_{10}$. A number of investigations of these alloys have shown that Fe-rich and Zr-rich alloys exhibit drastically different properties (Fe-rich samples, for example, are ferromagnetic and display Invar and spin-glass characteristics while Fe-poor samples are superconducting).[3–6] In addition to the liquid-quenched alloys, the vapor-deposition method has been used in several instances to prepare amorphous samples of noneutectic composition.[7–10]

Despite the relatively large number of investigations into a variety of properties of the amorphous Fe-Zr system, no systematic study of the magnetic properties and hyperfine interactions have been undertaken on samples prepared in a consistent fashion over the widest possible range of compositions. Indeed, the fact that a number of inconsistencies exist in the published data may be a reflection of this problem. Based on these considerations, the need is clear for a systematic study of the amorphous Fe-Zr system encompassing a very wide composition range and with particular emphasis on the intermediate compositions not available from liquid-quench techniques. In this work we report the results of such a study focusing on the magnetic properties and hyperfine interactions in a large number of amorphous alloys ranging in composition from $Fe_{20}Zr_{80}$ to $Fe_{93}Zr_7$.

## II. EXPERIMENTAL

Amorphous samples of $Fe_xZr_{100-x}$ ($20 \leq x \leq 93$) were prepared using a high-rate sputtering technique that has been more fully described elsewhere.[11] Sputtering targets were fabricated from homogeneous mixtures of pure Fe (99.9%) and pure Zr (99.8%). It was found that liquid-nitrogen-cooled substrates and reduced sputtering rates were necessary to produce amorphous Fe-rich and Zr-rich films. On the other hand, amorphous samples with intermediate compositions were easily obtained with room-temperature substrates and higher sputtering rates. In order to ensure consistent sample preparation conditions, all the results reported in this work were obtained using samples deposited onto liquid-nitrogen-cooled substrates of copper or Kapton at sputtering rates of about 0.05 $\mu$m/min.

In the case of those samples with Fe concentrations less than about 35 at. %, efficient substrate cooling during sputtering was found to be essential for producing amorphous samples due to the low crystallization temperatures of these alloys. When the amorphous state was not achieved, the resulting samples contained one or several of the metastable crystalline phases that have been reported in studies of the crystallization behavior of samples in this

 

composition range.[3,12,13] For comparison, liquid-quenched sample compositions of $Fe_{90}Zr_{10}$ and $Fe_{25}Zr_{75}$ were also studied.

Determination of the magnetic ordering temperatures as well as the hyperfine interactions were carried out on a conventional Mössbauer spectrometer ($^{57}$Co in Rh source). The thermal-scan method was used in the magnetic-ordering-temperature measurements.

## III. RESULTS AND DISCUSSION

### A. Composition range of amorphous samples

Vapor-deposited samples of $Fe_xZr_{100-x}$ in the range $20 \leq x \leq 93$ have been found to be amorphous. Samples prepared with greater or lesser Fe concentrations have been found to be partially or completely crystalline. When a $Fe_{95}Zr_5$ sample was deposited, for example, the resulting hyperfine interactions indicated the presence of at least two magnetic phases. One of these phases was consistent with the properties expected (based on an extrapolation of the properties of the single-phase amorphous samples) for an amorphous alloy of this composition. This sample, however, has not been included in the present discussion.

Restrictions on the available composition range of amorphous samples reflect the instability of elemental pure amorphous metals. This instability is indicated by the precipitous drop in the crystallization temperature as the elemental end points in an amorphous metallic alloy are approached.[14]

The fact that in the present case, pure Fe samples can be approached more closely (to 7 at. %) than pure Zr samples (to 20 at. %) is primarily a result of the difference in the respective atomic volumes. Egami and Waseda have reported a model in which the maximum ($x_{max}$) and minimum ($x_{min}$) compositions of a binary amorphous alloy can be determined.[15] Their approximate result applied to $Fe_xZr_{100-x}$ is

$$x_{min} \approx 10 \frac{V_{Zr}}{|\Delta V|} , \quad (1)$$

$$x_{max} \approx 100 - 10 \frac{V_{Fe}}{|\Delta V|} , \quad (2)$$

where $V_{Fe}$ and $V_{Zr}$ are the atomic volumes of Fe and Zr, respectively, and $|\Delta V| = |V_{Zr} - V_{Fe}|$. Using atomic radii of 1.24 and 1.60 Å for Fe and Zr, respectively,[16] one obtains $x_{min} \approx 19$ at. % and $x_{max} \approx 91$ at. %, in very good agreement with the experimental results.

### B. Magnetic ordering temperatures

The magnetic ordering temperatures ($T_c$) of the Fe-Zr samples are shown on the right-hand side of Fig. 1 as a function of Fe concentration. In each case the $T_c$ measurements were carried out on as-prepared samples.

Several qualitative features of the magnetic behavior of amorphous Fe-Zr are readily apparent. As in all other known amorphous alloys of Fe with an early transition metal (e.g., Fe-Nb, Fe-Ti ...), $T_c$ is found to be near or below room temperature for all compositions.[10,17] In addition, a clear maximum in $T_c$ is found at an Fe concentration of $x_p \approx 85$. Above $x_p$, $T_c$ decreases, and an extrapolation to $x = 100$ yields a value of $T_c$ in pure amorphous Fe of about 200 K. This result for amorphous pure Fe is consistent with similar extrapolations in other amorphous Fe containing binaries (Fe-B, Fe-Y).[11,18] At Fe concentrations less than $x_p$, $T_c$ decreases monotonically and essentially linearly before decreasing more gradually from $x \approx 55$ to the critical composition for magnetic ordering which occurs in the vicinity of $x_c \approx 45$. All samples with Fe concentrations less than $x_c$ show no signs of magnetic order, their Mössbauer spectra being simple quadrupole-split doublets at 4.2 K.

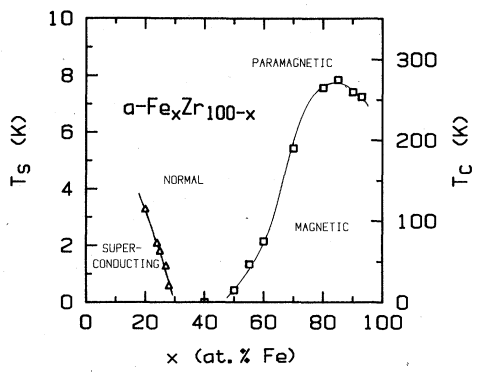


FIG. 1. Phase diagram of amorphous $Fe_xZr_{100-x}$ alloy system. The magnetic ordering temperatures ($T_c$) and the superconducting transition temperatures ($T_s$) are denoted, respectively, as squares and triangles. The values of $T_s$ are taken from Ref. 6.

The continuous diminution and final disappearance of the effective hyperfine field and therefore the Fe moment (as discussed in a later section), suggests that the magnetic threshold at a critical composition ($x_c$) is due to the loss of the Fe moment. Direct magnetization measurements are consistent with this conclusion; samples below $x_c$ being Pauli paramagnetic while samples above $x_c$ exhibit a finite moment.[8] A rapid decrease in $T_c$ leading to a magnetic threshold at $x_c$ has also been observed in a number of other amorphous Fe-$X$ ($X$ = B, Si, Nb, Ti, etc.) systems.[10,11,17,19]

A maximum in $T_c$ has also been found in other amorphous alloy systems. We have earlier reported a maximum in $T_c$ in amorphous $Fe_xB_{100-x}$, although the values of $T_c$ are much higher than in the present case.[11] Maxima are not found in those amorphous alloys in which the highest value of $T_c$ is less than about 200 K. In these systems (e.g., Fe-Ti, Fe-Nb), a monotonic increase in $T_c$ is observed in the Fe-rich samples.[11,17] These observations suggest that amorphous pure Fe is characterized by a unique and finite $T_c$ of about 200 K, instead of being nonmagnetic as some theories suggest.

A maximum in $T_c$ can be understood, at least qualitatively, within the framework of the localized moment or the itinerant pictures of magnetism. From a localized-moment standpoint, $T_c$ measures the net magnetic exchange interaction which must be decreasing. A decrease

in the coordination number (for fixed values of the exchange), a decrease in the strength of the ferromagnetic exchange due to a decrease in Fe-Fe spacing ($\partial J/\partial r > 0$), or the emergence of an antiferromagnetic exchange component could all be responsible for the observed behavior. A decrease in the coordination number at high Fe concentrations is unlikely in view of x-ray diffraction studies on an amorphous $Fe_{90}Zr_{10}$ alloy in which a coordination number of between 12 and 13 was found,[20] consistent with most other such results.

The itinerant picture has also been used to explain many of the observed properties of amorphous Fe containing alloys, including the maximum in $T_c$. Such a viewpoint postulates a magnetic phase diagram in which, with increasing Fe concentration, the magnetic properties of the amorphous alloy evolve from weak (holes in both $3d$ subbands) to strong (holes in only the minority subband) and back to weak ferromagnetism.[21] This approach also requires that the Fe moment decrease at sufficiently large concentrations. Earlier magnetization measurements in small applied fields (up to 15 kOe) have been interpreted as indicating just such a decrease in the Fe moments.[8,9,19] On the other hand, recent magnetization measurements under a very large applied field (up to 110 kOe) indicate a monotonically increasing Fe moment, a complete reversal of the low-field measurements.[22] These measurements, as well as our hyperfine-field measurements which also indicate a monotonically increasing Fe moment, will be discussed later. We feel that the observed composition dependence of $T_c$, particularly the maximum in $T_c$, can be most consistently explained in terms of the emergence of an antiferromagnetic exchange component.

### C. Superconductivity and magnetic order

A very interesting feature found in amorphous Fe-Zr alloys is the appearance of both superconductivity and magnetic order (although not at the same composition). This leads to the unusual phase diagram shown in Fig. 1. While magnetic order occurs in the Fe-rich samples, superconductivity appears in the Zr-rich samples. The rapid decrease in the superconducting transition temperature ($T_s$) with increasing Fe content, as shown in Fig. 1, has been explained in terms of the influence of spin fluctuations on $T_s$.[6] The strength of the spin fluctuations increases with Fe concentration, resulting in a rapid increase in the susceptibility. This precursor to magnetic order is responsible for the eventual destruction of the superconductivity. It is also interesting to note that for pure crystalline Zr, the value of $T_s$ is only about 0.6 K whereas substantially higher values were found in the amorphous Fe alloys, despite the large amounts of Fe present in these samples. By exhibiting both superconductivity and magnetic order, the amorphous Fe-Zr system is well suited for a study of the processes involved in the transition from superconductivity to magnetic order.

### D. Magnetic hyperfine interactions

Several magnetic Mössbauer spectra taken at 4.2 K of amorphous $Fe_xZr_{100-x}$ samples ranging in composition from $x = 93$ to 50 are shown in Figs. 2 and 3. The

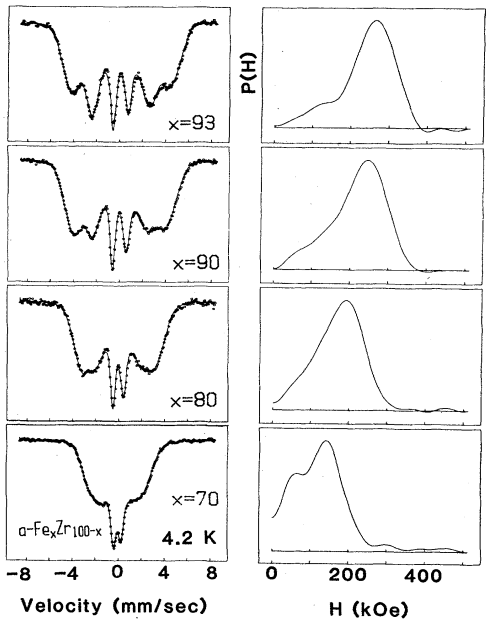


FIG. 2. Mössbauer spectra and the deduced hyperfine-field distribution [$P(H)$] of amorphous Fe-Zr at 4.2 K.

broadened spectral lines are characteristic of amorphous metallic alloys in which wide distributions of the internal fields are found. These spectra exhibit middle-line intensities $b$ (normalized so as to be in the ratio of 3:$b$:1) which are often less than 2, indicating that the magnetic moments are aligned substantially out of the sample plane. This effect is commonly observed in amorphous vapor-deposited ferromagnetic films at low temperatures and has been generally attributed to sample-substrate stresses

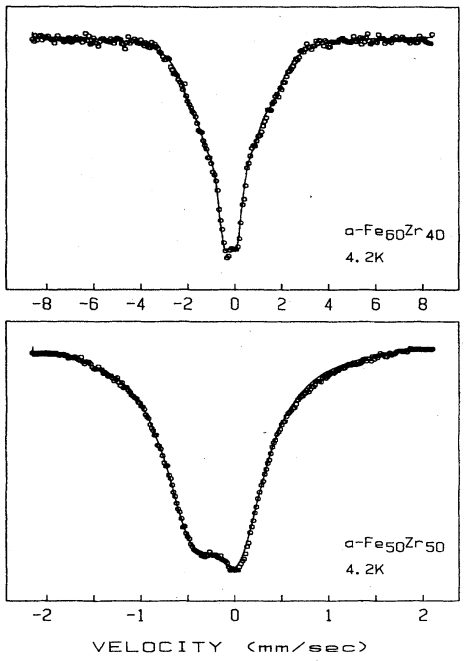


FIG. 3. Mössbauer spectra of amorphous $Fe_{60}Zr_{40}$ and $Fe_{50}Zr_{50}$ at 4.2 K. (Note the different velocity scales.)

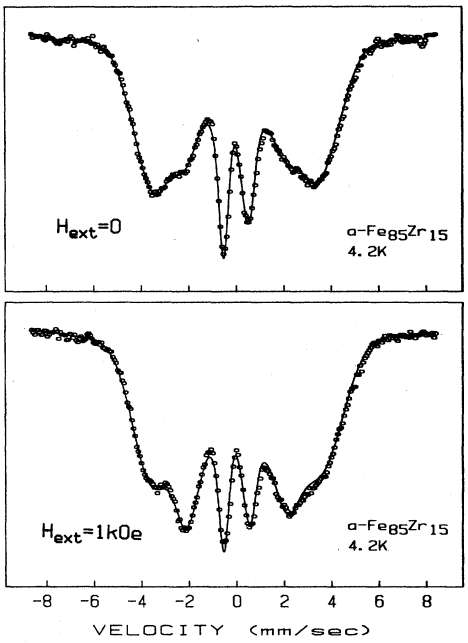


FIG. 4. Mössbauer spectra of amorphous $Fe_{85}Zr_{15}$ at 4.2 K with and without a small external field of about 1 kOe applied in the sample plane.

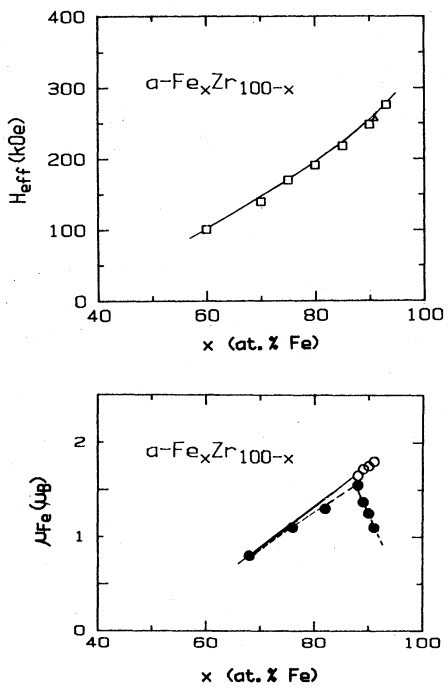


FIG. 5. Effective hyperfine field ($H_{\text{eff}}$) from Mössbauer measurements and the Fe magnetic moment ($\mu_{\text{Fe}}$) deduced from magnetization measurements of amorphous Fe-Zr alloys. In the upper figure, all values are taken from sputtered samples except one liquid-quench sample (triangle). In the lower figure, note the difference between the results from low-field (closed circles, from Ref. 19) and high-field (open circles, from Ref. 22) magnetization measurements.

arising during the deposition process or differences in sample-substrate thermal expansions.[23] By applying a small (about 1 kOe) external magnetic field in the sample plane, an increased spin alignment was achieved. An example is shown in Fig. 4 for an amorphous $Fe_{85}Zr_{15}$ sample. The ease with which the sample moments can be turned indicates that the magnetic ordering is largely ferromagnetic and rather soft.

It is apparent from Figs. 2 and 3 that the average splitting and the effective hyperfine field ($H_{\text{eff}}$) decrease with decreasing Fe concentration. In the case of $a$-$Fe_{50}Zr_{50}$ (bottom of Fig. 3; note the expanded velocity scale), the magnetic hyperfine splitting is so small that it appears as a broadened quadrupole doublet.

The composition dependence of the effective hyperfine field ($H_{\text{eff}}$) can be seen in Fig. 5. It is important to note that $H_{\text{eff}}$ is a monotonically increasing function of $x$ with no indication of a maximum as was seen in the $T_c$ data (see Fig. 1). Based on the well-documented, if approximate, proportionality between $H_{\text{eff}}$ and the Fe moment ($\mu_{\text{Fe}}$), one can conclude that $\mu_{\text{Fe}}$ also increases monotonically with $x$.[24] As mentioned earlier, several bulk magnetization measurements have indicated an unexpected decrease in the *magnetization* above about 88 at. % Fe.[8,9,19] If complete alignment of the Fe moments is achieved as assumed, the value of $\mu_{\text{Fe}}$ deduced from these measurements would show a corresponding decrease. This is shown in the lower graph of Fig. 5, in which the solid circles illustrate the data obtained by Ohnuma *et al.* from magnetization measurements under an external field of 10 kOe.[19] This decrease of $\mu_{\text{Fe}}$ would in fact extrapolate to $\mu_{\text{Fe}}=0$ in the case of pure amorphous Fe. However, if complete spin alignment is *not* achieved by the external field, the deduced $\mu_{\text{Fe}}$ would then be undervalued. The ample evidence for spin-glass behavior indicates a strong possibility of incomplete alignment of the moments under a modest field for these Fe-rich amorphous alloys.

Recently, high-field magnetization (up to 110 kOe) measurements have been performed by Hiroyoshi *et al.*[22] After correcting for the high-field susceptibility, the *saturation* magnetization is obtained. The deduced $\mu_{\text{Fe}}$, shown in the lower graph of Fig. 5 by the open circles, *completely reverses* the trend exhibited by the low-field data. The value of $\mu_{\text{Fe}}$ increases monotonically without anomaly as concluded readily by the hyperfine-field measurements shown in the upper graph of Fig. 5. Thus, based on both hyperfine-field measurements and high-field magnetization studies, amorphous pure Fe should be magnetic with a moment of about $2\mu_{\text{B}}$.

A consistent picture of the magnetic properties of Fe-rich amorphous Fe-Zr alloys can be achieved if one assumes the emergence of an antiferromagnetic exchange component at high Fe concentrations. Such an effect could explain the decrease in $T_c$, the difficulty in saturating the Fe moments in applied field experiments, the spin-glass and Invar-type behavior, and the presence of a low-field tail in $P(H)$ as will be discussed below.

The deduced hyperfine-field distributions [$P(H)$] obtained using a modification of Window's method[25] (assuming a linear correlation between the isomer shift and

the hyperfine field) are shown alongside the corresponding spectra in Fig. 2. The $P(H)$ of samples with Fe concentrations less than 70 at. % are not included due to the unreliability of the $P(H)$ fitting routine when the quadrupole splitting is no longer negligible with respect to the magnetic hyperfine splitting.

The hyperfine-field distributions are seen to be rather structureless, single maxima (the $a$-$Fe_{70}Zr_{30}$ sample, however, displays a prominent shoulder on the low-field side of the distribution) functions of $H$. In each case, the low-field side of the distribution decreases less rapidly than the high-field side. In addition, there is an indication of a low-field tail in the $P(H)$ of the amorphous $Fe_{93}Zr_7$ and $Fe_{90}Zr_{10}$ samples. Due to the asymmetry of these distributions, the mean hyperfine field is less than the most probable value of the hyperfine field.

A low-field tail on the hyperfine-field distribution is one characteristic feature of Invar behavior in crystalline materials.[26] Therefore, based on the $P(H)$ data, one might expect to also find such behavior in amorphous $Fe_{93}Zr_7$ and $Fe_{90}Zr_{10}$. Shirakawa has indeed reported an anomalously small coefficient of the thermal-expansion coefficient consistent with Invar behavior around room temperature in an amorphous $Fe_{90}Zr_{10}$ sample.[27]

### E. Isomer shifts and electric quadrupole splitting

Mössbauer spectra of various amorphous Fe-Zr alloys, taken at 300 K, are shown in Fig. 6. In each case, one observes a quadrupole split doublet, although in the case of the Fe-rich samples, the two peaks are poorly resolved. All the spectra can be well described by fitting the two peaks to two independent Lorentzian line shapes. The two peak positions then define the effective isomer shift ($\delta$) and the effective quadrupole splitting ($\Delta$).

The measured isomer shifts at 300 K, with respect to that of $\alpha$-Fe at room temperature, are shown as a function of composition in Fig. 7. While the room-temperature isomer shifts are all negative, as is typical of all amorphous Fe—early-transition metals, the quantitative dependence of $\delta$ on composition in the present case is somewhat different than that found in amorphous Fe-Nb and Fe-Ti.[17,28] In the latter cases, $\delta$ is characterized by a relatively rapid drop (more negative) with decreasing Fe content followed by a very shallow minimum. In Fe-Zr, two generally different regions, with the dividing point roughly at the equiatomic composition, have been found. In the Fe-rich region, the $\delta$-versus-$x$ curve is very similar to those found in the other Fe—early-transition-metal systems. In the Fe-poor region, however, rather than a shallow minimum, $\delta$ falls even more rapidly with no indication of a minimum to the lowest attainable compositions.

Miedema and van der Woude have obtained a semiempirical expression for the isomer shift, based on an earlier theory of the heats of formation, and applied it to a number of alloys.[29] The same model has been used by van der Kraan and Buschow in order to describe the isomer shifts in several amorphous Fe-containing alloys.[30]

The composition dependence of the isomer shift (relative to pure Fe) of $Fe_xZr_{100-x}$ using Miedema's model is

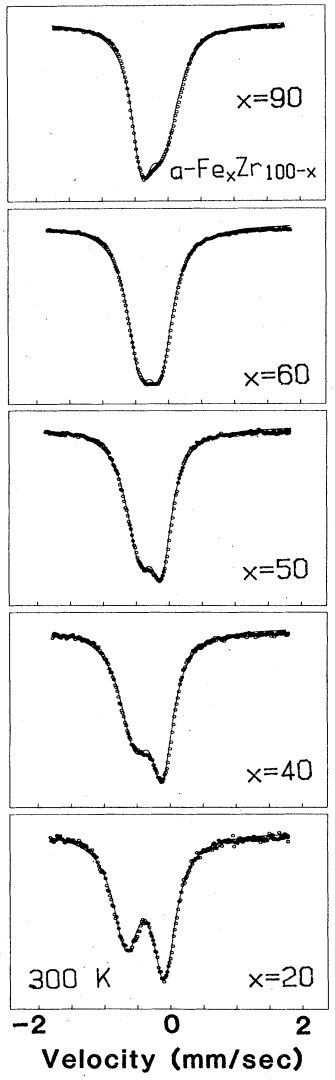


FIG. 6. Quadrupole spectra of amorphous Fe-Zr alloys at room temperature.

$$\delta(x)=\delta_{\mathrm{Fe,Zr}}\left[\frac{100-x}{100-x+x\left[\frac{V_{\mathrm{Fe}}}{V_{\mathrm{Zr}}}\right]^{2/3}}\right], \tag{3}$$

$$=\delta_{\mathrm{Fe,Zr}}[1-C_{\mathrm{Fe}}(x)]\,. \tag{4}$$

The first factor $\delta_{\mathrm{Fe,Zr}}$ gives the isomer shift of dilute Fe in Zr, i.e., $\delta(0)=\delta_{\mathrm{Fe,Zr}}$. The composition dependence $\delta(x)$ is determined entirely by the second factor, which is a monotonic function of $x$. The precise form of this monotonic function, and hence $\delta(x)$ depends only on the ratio of the atomic volumes $V_{\mathrm{Fe}}$ and $V_{\mathrm{Zr}}$. With this model, once the value of $\delta_{\mathrm{Fe,Zr}}$ is evaluated by either calculations as described below or by measuring the isomer shift of

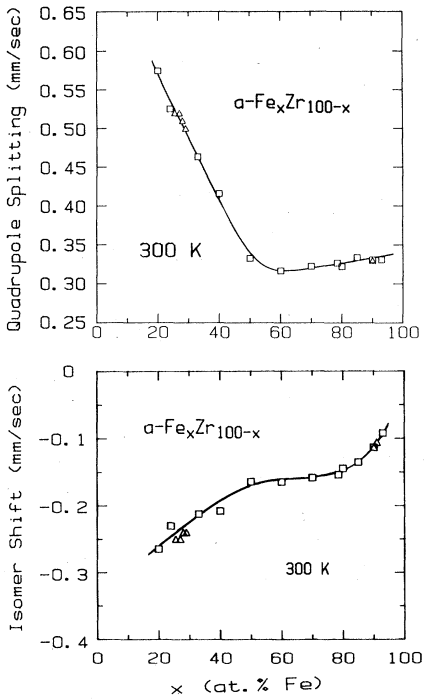


FIG. 7. Quadrupole splitting and isomer shift (relative to $\alpha$-Fe) of amorphous Fe-Zr alloys at room temperature. The squares and triangles are measured from sputtered and liquid-quench samples, respectively. The values of $x=27$, 28, and 29 are taken from Ref. 3.

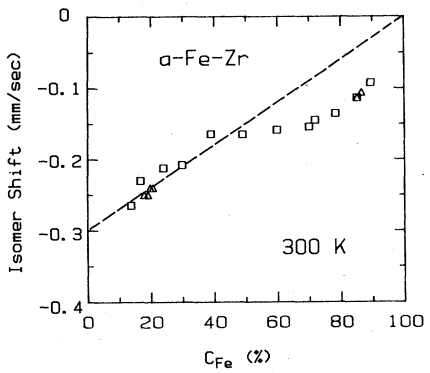


FIG. 8. Isomer shift of amorphous Fe-Zr alloys as a function of the effective concentration of $C_{Fe}$ defined in the text. The dashed line is the prediction by the model of Miedema and van der Woude.

only *one* composition, $\delta(x)$ as described by Eq. (3) is completely determined. In fact $\delta(x)$ should be linearly dependent on $C_{Fe}(x)$ as defined by Eq. (4).

According to Miedema, the value of $\delta_{Fe,Zr}$ can be calculated from

$$\delta_{Fe,Zr}=P(\phi_{Zr}-\phi_{Fe})+Q(n_{Zr}-n_{Fe})/n_{Fe}\ , \tag{5}$$

where $\phi$ and $n$ are the electronegativity and the electronic density at the boundary of the Wigner-Seitz cells characteristic of the pure elements. $P$ and $Q$ are two parameters for which best fit values have been obtained from a large class of Fe—transition-metal alloys. Extensive tabulation of the atomic volumes and the value of $\phi$ and $n$ can be found in Ref. 31. Using the tabulated values of $\phi_{Fe}=4.93$, $\phi_{Zr}=3.4$, $n_{Fe}=5.55$, $n_{Zr}=2.69$, $V_{Fe}^{2/3}=3.7$, and $V_{Zr}^{2/3}=5.8$, and the best-fit values of $P=0.75$ and $Q=-1.65$, one obtains $\delta_{Fe,Zr}=-0.30$ mm/sec.[30]

The values of $\delta$ versus $C_{Fe}(x)$ defined in Eqs. (3) and (4) are shown in Fig. 8. The dashed line represents the prediction using the above-mentioned values. Although it does not reproduce the detailed features found in the data, the qualitative agreement is very satisfactory. It is all the more remarkable considering the simplicity of the model.

The quadrupole splitting ($\Delta$), as shown in Fig. 7, illustrates the contrasting behavior between the Fe-rich and the Fe-poor samples. In the Fe-rich samples ($x\geq 50$), $\Delta$ has a weak compositional dependence, similar to other amorphous Fe—transition-metal alloys such as Fe-Ti and Fe-Nb.[17,28] The Fe-poor samples ($x\leq 50$) show an unexpected increase in $\Delta$ with a much stronger compositional dependence which is not observed in Fe-Ti or Fe-Nb. The anomalous behavior of both $\delta$ and $\Delta$ suggests that there are subtle changes in the structure of amorphous Fe-Zr between Fe-rich and Zr-rich samples. A detailed structural study of amorphous Fe-Zr across the entire available composition range would be most useful.

Finally, we comment on the amorphous samples made by liquid- and vapor-quench methods. As can be seen from Figs. 5 and 7, *no* appreciable difference in $\delta$, $\Delta$, or $H_{eff}$ can be observed between the sputter-deposited and liquid-quenched samples, despite very dissimilar quenching rates. Based on the very sensitive dependence of these quantities to subtle changes in the local atomic environments, one can conclude that the structures resulting from vapor quench and liquid quench are very similar.

## IV. SUMMARY AND CONCLUSIONS

In this work we have reported the results of a systematic study of the magnetic properties and hyperfine interactions as a function of composition in a large number of amorphous $Fe_xZr_{100-x}$ ($20\leq x\leq 93$) alloys. All of the samples have been prepared by high-rate sputter deposition and studied by $^{57}$Fe Mössbauer spectroscopy.

As is commonly found in Fe containing binary amorphous alloys, a critical Fe concentration ($x_c$) is required for magnetic order to first appear. In the present case, the critical Fe concentration is found to be about 45 at.%. Above $x_c$ the magnetic ordering temperature at first increases rather rapidly until an Fe concentration of about 85 at.% is reached and then decreases as the Fe concentration is increased still further. The ordering temperature of pure amorphous Fe is estimated to be about 200 K by extrapolation.

Unlike the concentration dependence of $T_c$, the effective hyperfine field exhibits a monotonic increase with Fe concentration. Despite the generally accepted proportionality between the hyperfine field and the Fe moment ($\mu_{Fe}$), several early magnetization studies of Fe-rich amor-

phous samples in relatively modest applied fields have been interpreted as indicating a maximum in $\mu_{Fe}$. Very recently, however, magnetization measurements have been reported in large applied fields. The results of these measurements indicate a monotonically increasing Fe moment, in agreement with our results, and demonstrating the usefulness of the microscopic Mössbauer effect in determining basic magnetic parameters.

Despite the fact that both localized and itinerant approaches to the problem of magnetism in general and amorphous magnetism in particular can explain many experimental observations, we feel that the monotonic increase in the Fe moment to the most Fe-rich amorphous alloys obtainable is of importance. The absence of a maximum in $\mu_{Fe}$ argues against the itinerant electron picture and in favor of a more localized approach. From this viewpoint the experimentally observed behavior of both $T_c$ and $\mu_{Fe}$ can be reconciled by assuming the emergence of an antiferromagnetic exchange interaction. Such a model also accounts for other magnetic properties such as the Invar and spin-glass behavior.

The quadrupole splitting and the isomer shift are unexpectedly different for the Fe-rich and the Fe-poor samples, suggesting a subtle but significant change in the structure.

## ACKNOWLEDGMENTS

We thank Dr. K. Fukamichi for supplying the liquid-quench samples. This work was supported by the National Science Foundation under Grant No. DMR-82-05135.

---

*Present address: W. M. Keck Laboratory of Engineering Materials, California Institute of Technology, Pasadena, CA 91125.

[1]See, e.g., H. H. Lieberman, in *Amorphous Metallic Alloys,* edited by F. E. Luborsky (Butterworths, London, 1983), pp. 26—41.

[2]See, e.g., *Handbook of Thin Film Technology,* edited by L. I. Maissel and R. Glang (McGraw-Hill, New York, 1970).

[3]M. Ghafari, U. Gonser, H.-G. Wagner, and M. Naka, Nucl. Instrum. Methods **199**, 197 (1982).

[4]K. Fukamichi, in *Amorphous Metallic Alloys,* edited by F. E. Luborsky (Butterworths, London, 1983), pp. 317—340.

[5]H. Hiroyoshi and K. Fukamichi, Phys. Lett. **85A**, 242 (1981).

[6]Z. Altounian and J. O. Strom-Olsen, Phys. Rev. B **27**, 4149 (1983).

[7]N. Heiman and N. Kazama, Phys. Rev. B **19**, 1623 (1978).

[8]K. H. J. Buschow and P. H. Smit, J. Magn. Magn. Mater. **23**, 85 (1981).

[9]K. Fukamichi and R. J. Gambino, IEEE Trans. Magn. **MAG-17**, 3059 (1981).

[10]K. M. Unruh and C. L. Chien, J. Magn. Magn. Mater. **31-34**, 1578 (1983).

[11]C. L. Chien and K. M. Unruh, Phys. Rev. B **25**, 5790 (1982).

[12]I. Vincze, F. van der Woude, and M. G. Scott, Solid State Commun. **37**, 567 (1981).

[13]H. U. Krebs, C. Michaelsen, J. Reichelt, H. A. Wagner, J. Wecker, Q. R. Zhang, and H. C. Freyhardt, in *Liquid and Amorphous Metals V,* edited by C. N. J. Wagner and W. L. Johnson (North-Holland, Amsterdam, 1984), pp. 463—468.

[14]K. H. J. Buschow, J. Less-Common Met. **79**, 243 (1981).

[15]T. Egami and Y. Waseda, J. Non-Cryst. Solids **64**, 113 (1984).

[16]See, e.g., *Lange's Handbook of Chemistry,* 12th ed., edited by J. A. Dean (McGraw-Hill, New York, 1979), pp. 3—120.

[17]S. H. Liou and C. L. Chien, J. Appl. Phys. **55**, 1820 (1984).

[18]J. Chappert, T. Abbese-Boggiano, and J. M. D. Coey, J. Magn. Magn. Mater. **7**, 175 (1978).

[19]S. Ohnuma, K. Shirakawa, M. Nose, and T. Masumoto, IEEE Trans. Magn. **MAG-16**, 1129 (1980).

[20]H. S. Chen, K. T. Aust, and Y. Waseda, J. Non-Cryst. Solids **46**, 307 (1981).

[21]E. P. Wohlfarth, in *Amorphous Metallic Alloys,* edited by F. E. Luborsky (Butterworths, London, 1983), pp. 283—299.

[22]H. Hiroyoshi and K. Fukamichi, in *High Field Magnetism,* edited by M. Date (North-Holland, Amsterdam, 1983).

[23]H. N. Ok and A. H. Morrish, Phys. Rev. B **22**, 4215 (1980).

[24]See, e.g., P. Panissad, J. Durand, and J. I. Budnick, Nucl. Instrum. Methods **199**, 99 (1982).

[25]B. Window, J. Phys. E **4**, 401 (1971).

[26]U. Gonser, S. Nasu, W. Keune, and O. Weiss, Solid State Commun. **17**, 233 (1975).

[27]K. Shirakawa, S. Ohnuma, M. Nose, and T. Masumoto, IEEE Trans. Magn. **MAG-16**, 910 (1980).

[28]C. L. Chien, K. M. Unruh, and S. H. Liou, J. Appl. Phys. **53**, 7756 (1982).

[29]A. R. Miedema and F. van der Woude, Physica (Utrecht) **100B**, 145 (1980).

[30]A. M. van der Kraan and K. H. J. Buschow, Phys. Rev. B **25**, 3311 (1981); **27**, 2693 (1983).

[31]A. R. Miedema, J. Less-Common Met. **41**, 283 (1975); **46**, 67 (1976).